

X-Ray Diffraction Studies of Uranyl Hydrolysis Precipitates Synthesized in Neutral to Alkaline Aqueous Solutions

Yong Joon Park, Hyung Yeal Pyo, Won Ho Kim, and Kwan Sik Chun

Korea Atomic Energy Research Institute, Taejon 305-606, Korea

Received June 19, 1996

Uranyl hydrolysis precipitates were obtained by increasing pH value of aqueous uranyl solution in the range of neutral to alkaline pH value and their phase transformation during the solubility experiment under various conditions has been examined. The precipitates formed in the hydrolysis reaction of uranyl ion had a layered structure such as a meta-schoepite phase, a schoepite structure, or a mixed phase of meta-schoepite and schoepite. Phase transformation between them was strongly dependent on the pH value at which the precipitate was formed. The distance between the layers in meta-schoepite or schoepite phase was $\sim 7.35 \text{ \AA}$, and it was increased with the pH value at which the precipitate was synthesized as well as the pH values of the aqueous solution. The phase transformation from a meta-schoepite to schoepite was fast for the precipitates formed at low pH values, however, it was not the case for the precipitates formed at high pH values. A small difference of pH value in aqueous solution gave a great change on its solubilities near pH 9.7, because a layered structure of the precipitates became amorphous above that pH value. Greater solubility for the precipitate formed at higher pH value can be explained from the fact that the precipitates formed at low pH value had a better crystallinity and also that the precipitates formed at higher pH value has a slower rate of crystallization.

Introduction

Nuclear fuel waste disposal is the final stage of the nuclear energy cycle, and is intended to keep man and the environment safe from the hazardous wastes. The isolation of the high-level nuclear wastes and the integrity of the vault are expected to be such that the only feasible mechanism for escape of radioactive material would be transport of radionuclides through the intrusion of groundwater from a potential nuclear waste repository to the accessible environment. The magnitude of the contamination is controlled by the dissolution rate of the waste package, the formation of solubility-controlling solids, and the formation of soluble species.

Uranium is the major constituent of high-level nuclear waste. The solubilities of the hydrated uranyl hydroxides as well as their related compounds in solution are of major importance and have received much attention. Uranyl hydrolysis precipitates (schoepite type phases) have been identified as a primary concern in dissolution studies of crystalline UO_2^1 and as a possible precipitate in leaching studies of irradiated UO_2 fuel² in air-saturated solutions.

As it is commonly accepted, the solubility of a solid is strongly dependent on its morphology. In this sense, the solubility of an amorphous phase provides values which, in some sense, can be several orders of magnitude higher than those obtained in a crystalline phase.³ Therefore, the solids formed from the over-saturation in solubility tests must be clearly identified by physical or chemical characterization methods. Radionuclide solids formed in laboratory experiments and in nature are often thermodynamically ill-defined amorphous precipitates. Most amorphous solids, however, will become more crystalline with time.⁴

In this context, the aim of this work is to identify and characterize the solid phases of uranyl hydrolysis precipitates that could be formed in neutral to alkaline solution, as well

as their transformation during the solubility experiment under the various conditions. Solubility test of the precipitates were also investigated at different stage of the experiments, however, the solubility data will not be discussed here.

Experimental

CO_2 -free NaOH and HCl solutions used in this study were of analytical grade (J. T. Baker). All other solutions were prepared with CO_2 -free distilled deionized water obtained by boiling deionized water from a Milli-Q plus system while purging with nitrogen gas.

U(VI) stock solution were made by dissolving UO_2 powder into 6 M HClO_4 , keeping pH of solution at 2 with ammonia water. Hydrogen peroxide solution (30%) was added into the solution until formation of uranyl peroxide precipitates stopped. Solutions were filtered with Whatman filter paper (No. 42) and the filtered materials were dissolved into 1.0 M HCl. Solutions were heated to remove residual hydrogen peroxides and were subsequently diluted to appropriate volume with CO_2 -free distilled deionized water. Solutions were then standardized by titration with $\text{K}_2\text{Cr}_2\text{O}_7$ solution.

Solid hydrated uranyl hydroxides ($\text{UO}_3 \cdot 2\text{H}_2\text{O}$, chemically equivalent to $\text{UO}_2(\text{OH})_2 \cdot \text{H}_2\text{O}$) were precipitated from a solution of uranyl chloride by adding dropwise a 1 M CO_2 -free NaOH solution under constant $\text{N}_2(\text{g})$ stream at room temperature. The pH of the solution was repeatedly measured during the precipitation process. After separation of the precipitates from its mother liquid by centrifuging, the solid was thoroughly washed with CO_2 -free distilled deionized water. This solid phase was transferred to a vessel for the solubility test that took about 1 to 4 weeks. The initial and the final products obtained from the experiment were dried under $\text{N}_2(\text{g})$ atmosphere and then characterized by X-ray powder diffraction (XPD) and SEM micrographs. XPD data were then

analyzed to obtain the crystal lattice parameters using the Siemens WIN-INDEX and WIN-METRIC programs.

The XPD patterns were recorded on a Siemens model D5000 diffractometer, using a CuK α radiation ($\lambda=1.540562$ Å). The 2θ scan rate was $2.4^\circ \text{ min}^{-1}$, the current 30 mA and the voltage 40 kV. The "low-angle-cut-off" for the instrument is $2\theta=2^\circ$. The diffraction patterns were normally taken in the range of $10^\circ \leq 2\theta \leq 40^\circ$. The solid phases were also examined by scanning electron microscopy (SEM), in a LEICA-S360 scanning electron microscope.

Description of samples All the samples used were collected from the solubility experiments with uranyl hydrolysis precipitates (denoted as UHPs) which were synthesized at pH 6.4 and 9.4, respectively. Solubility tests of two different types of precipitates in sulfate or bicarbonate solution were conducted under the various pH conditions. The concentration of sulfate and bicarbonate used in the experiment were 1.00×10^{-4} M and 1.25×10^{-3} M, respectively. Solubility tests of UHPs were also carried out in various concentration of bicarbonate solutions ($0 \sim 2.2 \times 10^{-3}$ M). In this case, the pH of the solution were varied according to the concentration of bicarbonate.

-UHP-9.4-BC-pH series: Powder samples collected from the solubility experiment in bicarbonate solution (pH 8.45 to 5.87) with the uranyl hydrolysis precipitate synthesized at pH 9.4.

-UHP-6.4-BC-pH series: Powder samples collected from the solubility experiment in bicarbonate solution (pH 9.70 to 5.70) with the uranyl hydrolysis precipitate synthesized at pH 6.4.

-UHP-6.4-S-pH series: Powder samples collected from the solubility experiment in sulfate solution (pH 10.48 to 5.66) with the uranyl hydrolysis precipitate synthesized at pH 6.4.

-UHP-9.4-S-pH series: Powder samples collected from the solubility experiment in sulfate solution (pH 9.54 to 5.76) with the uranyl hydrolysis precipitate synthesized at pH 9.4.

-UHP-6.4-BC-CON series: Powder samples collected from the solubility experiment in various concentration of bicarbonate solution (0 to 2.2×10^{-3} M) with the uranyl hydrolysis precipitate synthesized at pH 6.4.

-UHP-6.4-S-CON series: Powder samples collected from the solubility experiment in various concentration of sulfate solution (0 to 5.00×10^{-4} M) with the uranyl hydrolysis precipitate synthesized at pH 6.4.

Results and Discussion

Uranyl hydrolysis precipitates were obtained as a precipitate form when increasing pH value of aqueous uranyl solution in the range of neutral to alkaline pH. The crystal structure, the degree of crystallinity and the solubility of these UHPs are strongly dependent on what pH value the precipitate was formed. These factors can lead to a large uncertainty in predicting its solubility. As increasing the pH value of aqueous uranyl solution by adding CO₂-free NaOH solutions dropwise, the pale yellow fine-grained solid precipitate started forming at pH 4.5 in solution. The color of the precipitates became darker to yellow at the pH region 7 to 10, and consequently to orange above pH 10.5. The XPD pattern indicates that the precipitates of orange are amorphous.

The precipitates formed in the hydrolysis reaction of ura-

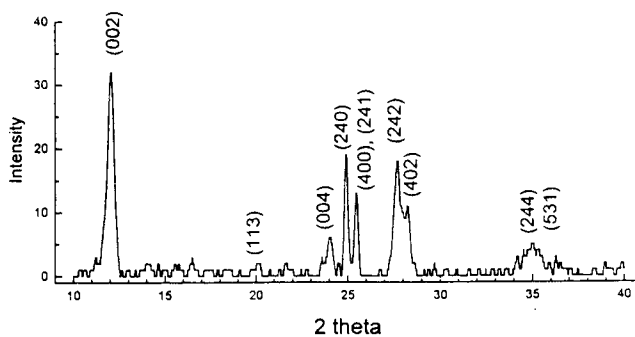


Figure 1. X-ray powder diffraction pattern of UHP (meta-schoepite phase).

nyl ion in aqueous solution are generally known as schoepite with composition of UO₃·2H₂O. According to Christ and Clark⁵, crystals of schoepite yield multiple diffraction patterns that correspond to the presence of three possible orthorhombic phases in parallel intergrowth in the crystal. The three phases are designated schoepite I, II and III, which are generally called schoepite, meta-schoepite and para-schoepite, respectively. The powder diffraction file (card no. 18-1436) in the Joint Committee on Powder Diffraction Studies (JCPDS) showed that schoepite II (meta-schoepite) represents apparently an intermediate stage of alteration.⁶ It was also mentioned that schoepite I may contain water more than two molecules and schoepite II and III may contain water less than two molecules.

The XPD pattern of the initial precipitates obtained at pH ranges from 6 to 10 showed the presence of peaks corresponding to a microcrystalline hydrated uranyl hydroxides phase (schoepite II) referring to the JCPDS card no. 18-1436 (see Figure 1). This phase undergoes transformation into schoepite I within a certain period that depends on pH values where the precipitate was formed. The XPD pattern corresponding to schoepite III phase, however, was not observed during the entire experiments. Figure 2 shows the XPD pattern (schoepite I, referring to the JCPDS card no. 13-0241) of the precipitates synthesized at pH 6.4 after allowing them for one week in sulfate solution, which indicates the phase transformation from schoepite II to schoepite I. However, this phase transformation was not observed for the precipitates synthesized at pH 9.4 after allowing them for one week in sulfate or bicarbonate solution. It was also observed that either sulfate or bicarbonate species in aqueous solution did not cause any other phase transformations to uranyl sulfate hydrate or uranyl carbonate hydrate, etc. within a week period.

As shown in Figure 1 and Figure 2, the first two sharp peaks observed near 12 and 24° for the both phases were assigned by the Miller indices of (002) and (004), respectively, which could indicate layered structure. The distance between the layers in meta-schoepite or schoepite phase was around 7.35 Å. The SEM micrographs obtained (see Figure 3(a)) showed the tabular morphology characteristic of this phase. The hkl values obtained using WIN-INDEX and WIN-METRIC programs were in good agreement with those reported in the JCPDS powder diffraction file.

As can be seen in Figure 4, the degree of crystallinity decreased markedly as a function of the pH values at which

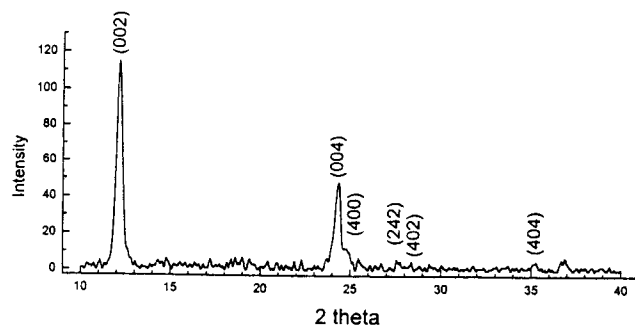
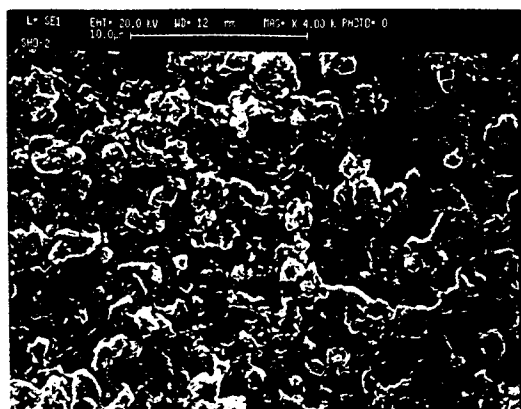
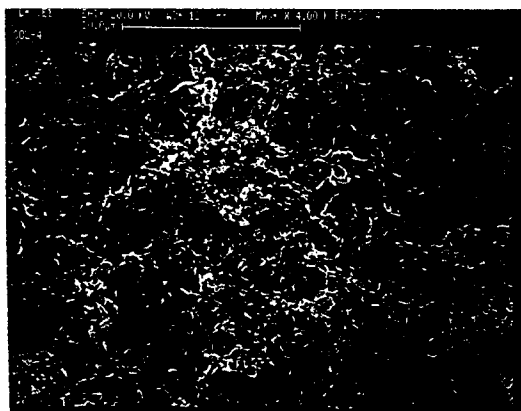


Figure 2. X-ray powder diffraction pattern of UHP (schoepite phase).



(a)



(b)

Figure 3. SEM micrographs of uranyl hydrolysis precipitates synthesized at (a) pH 9.4 and (b) pH 9.7 (magnification $\times 8000$).

the UHP was formed. Consequently, this trend leads to an amorphous XPD pattern (Figure 4(a)) for the precipitates synthesized at pH 11. The SEM micrographs of the UHPs synthesized at pH 9.4 and 9.7 were compared in Figure 3. The XPD patterns of these UHPs were shown in Figure 4(b) and (c). The SEM micrograph of UHP synthesized at pH 9.7 apparently showed the indication of the destruction of tabular structure of metaschoepite phase by comparing with that of UHP synthesized at pH 9.4, as indicated in the corresponding XPD patterns. These informations together with the corresponding XPD patterns lead to the conclusion that the pH value of 9.7 seems to be the critical pH boundary

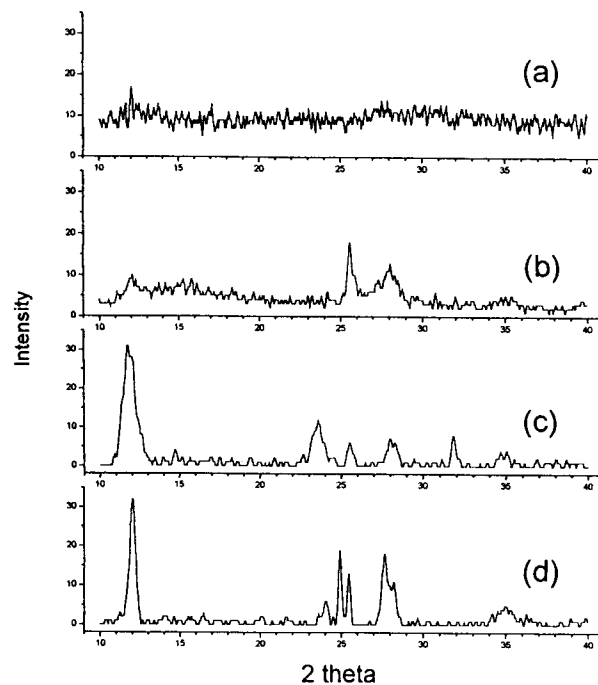


Figure 4. Comparison of X-ray powder diffraction patterns of UHPs synthesized at (a) pH 10.0 (b) 9.7 (c) 9.4 (d) 6.4.

at which a layered structure of the precipitates collapses and becomes amorphous. Therefore, a small difference of pH value above pH 9.7 in aqueous solution in which the precipitates was formed provided a great change on its crystallinity. As a backup for this result, the experimental data of the solubility test with these precipitates also showed a great change on their solubilities.

The shift of (002) and (004) peaks to lower scattering angle was observed in Figure 4 as increasing the pH values where the precipitate was formed. This information in the XPD patterns indicates straightforwardly that the thickness of the unit layer (d_{002}) increases with the pH values at which the precipitate was synthesized.

A similar result was seen from the XPD patterns of UHPs obtained after the solubility experiments of UHPs under various pH conditions of bicarbonate or sulfate solution. Figure 5 and Figure 6 show the XPD patterns of UHPs synthesized at pH 9.4 and 6.4 from the solubility experiment in carbonate solutions of various pH values, respectively. The XPD patterns of UHP formed at pH 9.4 shown in Figure 5 were identified as the meta-schoepite phase, while the XPD patterns shown in Figure 6 were as the schoepite phase, as mentioned earlier. As can be seen in both Figure 5 and 6, (002) and (004) peaks of UHPs were shifted to higher scattering angle as the pH of the solution decreased. The XPD patterns of UHPs obtained from the solubility experiment in sulfate solutions of various pH values also showed same trend, however, the XPD patterns of UHPs in various concentration of sulfate solutions did not show a peak shift for (002) or (004). It can be concluded from this fact that the thickness of schoepite or meta-schoepite phase is not affected by the chemical species present in the solution, but the pH values of the solution. In addition to that, one or more peaks for (002) and (004) were observed at the pH ranges from 6.00

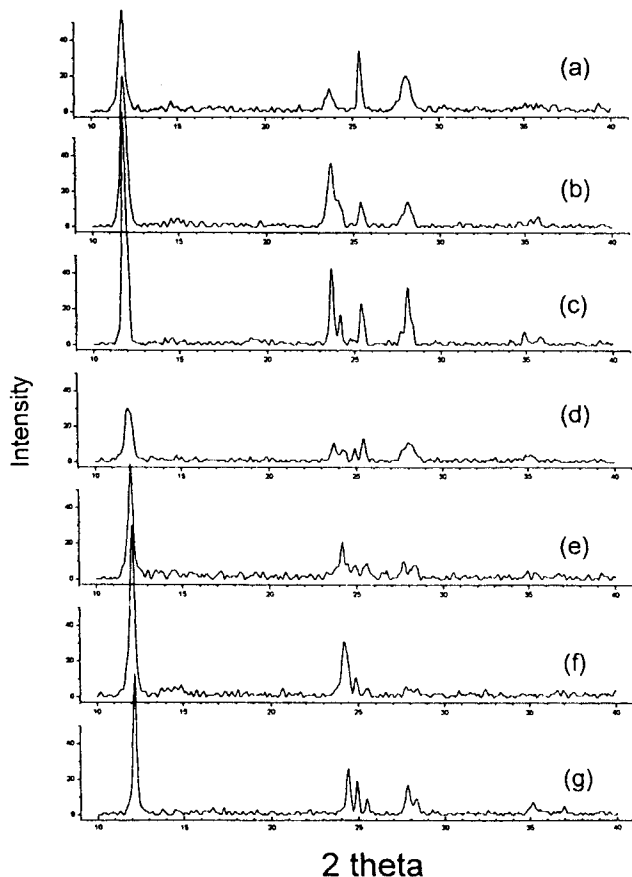


Figure 5. X-ray powder diffraction patterns of UHPs synthesized at pH 9.4 from solubility experiment in carbonate solution of (a) pH 8.45 (b) pH 7.46 (c) pH 7.11 (d) pH 7.10 (e) pH 7.02 (f) pH 6.65 (g) pH 5.87.

to 9.00, which indicates the presence of several different phases that have a different layer thickness.

A detailed peak shape and scattering angle position of (002) was shown in Figure 7 for the UHPs obtained from the various solubility experiments with a different matrix of the solution. The pH value of the bicarbonate solution for UHP-6.4-BC-CON 6.3×10^{-4} (see Figure 7(f)) measured were 8.29. Figure 7 shows that the scattering angle position of (002) for the UHPs obtained from the various solubility experiments was shifted toward lower angle as increasing the pH values of the solution, even though the precipitates were synthesized at a different pH value. The expansion of unit cell may be due to the insertion of water molecules into the layered structure. Therefore, the expansion of unit cell for UHP is not influenced by the matrix of the solution but the pH condition of the aqueous solution where the UHP is in equilibrium.

The presence of more than single phase in the UHPs may explain the development procedure of cell expansion process. As soon as the pH value of the solution changes by adding acid or base, the unit cell of schoepite or meta-schoepite phase starts to expand or contract. The magnitude of the expansion of unit cell which results in the shift of (002) peak depends on the equilibrium pH value of the experiment solution. Therefore, the presence of more than a single phase

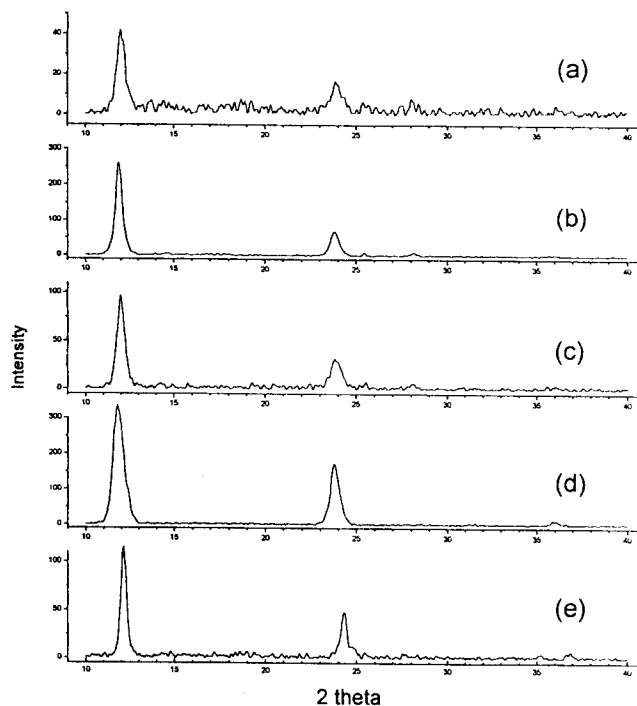


Figure 6. X-ray powder diffraction patterns of UHPs synthesized at pH 6.4 from solubility experiment in carbonate solution of (a) pH 9.7 (b) pH 8.6 (c) pH 7.1 (d) pH 6.6 (e) pH 5.7

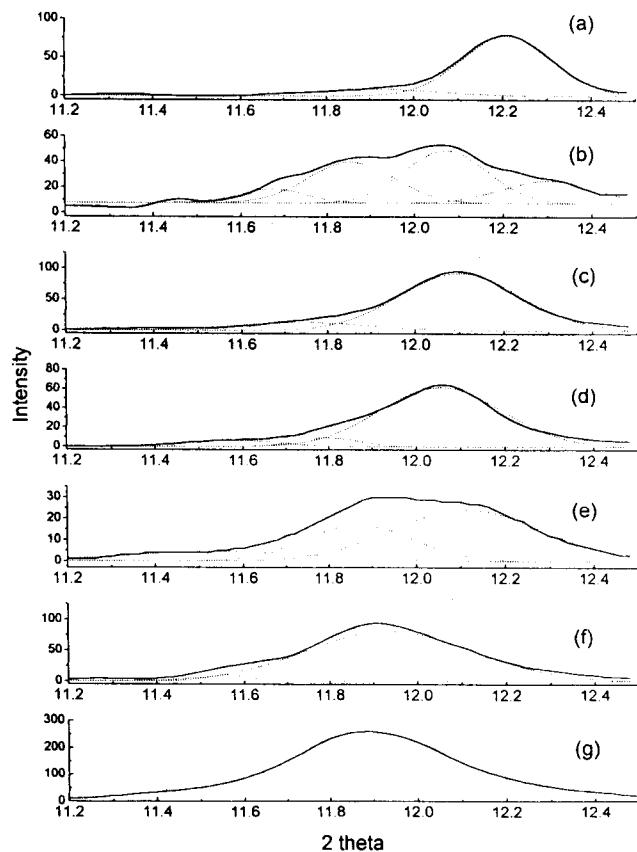


Figure 7. X-ray powder diffraction maxima ($d_{(002)}$) for the following sample: (a) UHP-9.4-BC-pH 5.87 (b) UHP-9.4-S-pH 6.06 (c) UHP-9.4-BC-pH 6.6 (d) UHP-9.4-BC-pH 7.02 (e) UHP-9.4-BC-pH 7.10 (f) UHP-6.4-BC-CON 6.3×10^{-4} (g) UHP-6.4-BC-pH 8.60.

in the precipitates from the experiment of pH range from 6.00 to 9.00 indicates that some of the crystal cells of the precipitate have been in equilibrium with a different pH before reaching the final pH of solution, since cell expansion process takes a certain amount of time.

As a conclusion, X-ray diffraction pattern for the precipitate in uranyl hydrolysis reaction was strongly dependent on the pH values, where their precipitates were formed as well as where the precipitates are in equilibrium with. A layered structure of the precipitates became amorphous when the precipitate were formed at pH >9.7. Greater solubility for the precipitate formed at higher pH value can be explained from the fact that the precipitates formed at lower pH value had a better crystallinity and also that the precipitates formed at higher pH value has a slower rate of crystallization. The thickness of the unit layer of UHPs increases with the pH values at which the precipitate was synthesized

as well as the pH values of the solution.

References

1. Wang, R. *Spent Fuel Special Studies Progress Report: Probable Mechanisms for Oxidation and Dissolution of Single-Crystal UO₂ surfaces*, PNL-3566, Pacific Northwest Laboratory, Richland, Washington, 1981.
2. Vandergraaf, T. T. *Leaching of Irradiated UO₂ Fuel*, Technical Record TR-100, Whiteshell Nuclear Research Establishment, Pinawa, Manitoba, Canada, 1980.
3. Bruno, J.; Casas, I.; Lagerman, B.; Munoz, M. *Mat. Res. Soc. Symp. Proc.* **1987**, *84*, 153.
4. Nitsche, H. *Radiochimica Acta* **1991**, *52/53*, 3.
5. Christ, C. L.; Clark, J. R. *Am. Mineral.* **1960**, *45*, 1026.
6. *Joint Committee on Powder Diffraction Standards, Powder Diffraction File Sets 11-15* (revised), p 480.

Redox Chemistry and Autoreduction of Non- μ -oxo Dimer-Forming [5,10,15,20-Tetrakis(2,6-dichlorophenyl)porphyrinato] Manganese(III) Chloride by Hydroxide Ion

Seungwon Jeon*, Hyo Kyoung Lee, and Yong-Kook Choi

Department of Chemistry, Chonnam National University, Kwang-ju 500-757, Korea

Received June 26, 1996

The electrochemistry and the reaction of non- μ -oxo dimer-forming [5,10,15,20-tetrakis(2,6-dichlorophenyl)porphyrinato] manganese(III) chloride [(Cl₂TPP)Mn^{III}Cl] with tetraethylammonium hydroxide in water [OH(H₂O)] have been investigated by electrochemical and spectroscopic methods under anaerobic conditions. The stronger autoreduction of (Cl₂TPP)Mn^{III}Cl by OH(H₂O) in comparison with (Me₁₂TPP)Mn^{III}Cl by OH(CH₃OH) in MeCN is explained as the influence of electronic effects on substituted phenyl groups bonded to *meso*-position of porphyrin ring and the positive shift of reduction potential (-0.11 V) for (Cl₂TPP)Mn^{III}Cl. The autoreduction of manganese(III) porphyrin to manganese(II) by this process is only observed when one axial position is occupied by a ligating solvent and OH coordinates the other axial site. The results are discussed in relation to the mechanisms for the reduction of manganese(III) porphyrin.

Introduction

Metalloporphyrins can experience reversible redox reactions in which the site of electron transfer may be localized at either the central metal or the porphyrin ring. Manganese porphyrins have several interesting aspects of physical, chemical, and biological properties which distinguish them from other metalloporphyrins.¹⁻³ Manganese porphyrins continue to be of interest as models for the behavior of cytochrome P-450,⁴⁻⁵ photosystem II,⁶⁻⁷ and superoxide dismutase,⁸ as DNA binding and cleavage reagents,⁹⁻¹¹ and as catalysts for the epoxidation of olefins.¹²⁻¹⁶ Axial ligation of manganese porphyrins coupled with redox chemistry is very important in diverse biological functions.¹⁷⁻²²

Electrochemical studies on the redox properties of manganese porphyrins are numerous.²³⁻²⁷ Manganese porphyrins

have been studied by electrochemical methods in the fields of electron transfer kinetics and ligand addition reactions,²⁸⁻²⁹ counterion and solvent effects,³⁰⁻³¹ and porphyrin substituent effects.³²

A kind of metalloenzyme containing manganese as a core metal mediates the oxidation of water to dioxygen in green plant photosynthesis by variations in its oxidation and ligation states.³³⁻³⁴ The oxidation of water to produce dioxygen is presumably less understood. It was recently reported that the reaction of manganese(III) tetramesitylporphyrin with excess methanolic hydroxide ion [OH(CH₃OH)] in ligating and nonligating solvents resulted in the formation of manganese(II) which in a slower reaction is oxidized to manganese(III).³⁵⁻³⁶ The mechanism for the oxidation of manganese(II) to manganese(III) is still ambiguous. In that report, because methanolic hydroxide ion is used, manganese(II) can be oxi-